ЖЭТФ, 2021, том 159, вып. 4, стр. 598–606

A DZYALOSHINSKII – MORIYA INTERACTION GUIDE TO MAGNETS MICRO-WORLD

V. V. Mazurenko [a*], ***Y. O. Kvashnin*** [b], ***A. I. Lichtenstein*** [c,a], ***M. I. Katsnelson*** [d,a]

[a] *Theoretical Physics and Applied Mathematics Department, Ural Federal University 620002, Ekaterinburg, Russia*

[b] *Uppsala University, Department of Physics and Astronomy, Division of Materials Theory SE-751 20, Uppsala, Sweden*

[c] *I. Institut für Theoretische Physik, Universität Hamburg D-20355, Hamburg, Germany*

[d] *Institute for Molecules and Materials, Radboud University NL-6525, AJ Nijmegen, The Netherlands*

Received December 4, 2020,
revised version December 4, 2020
Accepted for publication December 4, 2020

Contribution for the JETP special issue in honor of I. E. Dzyaloshinskii's 90th birthday

DOI: 10.31857/S0044451021040039

Abstract. Dzyaloshinskii–Moriya interaction (DMI) represents an antisymmetric type of magnetic interactions that favour orthogonal orientation of spins and competes with Heisenberg exchange. Being introduced to explain weak ferromagnetism in antiferromagnets without an inversion center between magnetic atoms such an anisotropic interaction can be used to analyze other non-trivial magnetic structures of technological importance including spin spirals and skyrmions. Despite the fact that the corresponding DMI contribution to the magnetic energy of the system has a very compact form of the vector product of spins, the determination of DMI from first-principles electronic structure is a very challenging methodological and technical problem whose solution opens a door into the fascinating microscopic world of complex magnetic materials. In this paper we review a few such methods developed by us for calculating DMI and their applications to study the properties of real materials.

1. Introduction. In a seminal paper [1] I. E. Dzyaloshinskii has introduced a novel type of anisotropic magnetic interactions which are antisymmetric with respect to swapping the positions of two spins. This was done based on a purely phenomenological basis. Very soon, Moriya [2] suggested the first simplified microscopic explanation of these interactions, indirect exchange and spin-orbit coupling (SOC) being the key ingredients. The Hamiltonian governing these interactions can be written in the following form:

$$\hat{H}_{DMI} = \sum_{i,j} \mathbf{D}_{ij}[\hat{\mathbf{S}}_i \times \hat{\mathbf{S}}_j], \tag{1}$$

where $\mathbf{S}_i$ is the spin moment at the site i. Nowadays the parameter $\mathbf{D}_{ij}$, which is, by construction, an axial vector, is known as Dzyaloshinskii – Moriya interaction.

"Slow is the experience of all deep fountains: long have they to wait until they know what has fallen into their depths." (F. Nietzsche).

Whereas the first decades DMI were considered as more or less marginal subject in magnetism (with the only exception of the phenomenon of weak ferromagnetism) now they are the mainstream subject, of a great conceptual meaning and of a great practical importance [3–8]. This only contribution would be sufficient to put the name of Igor Dzyaloshinskii among the main creators of modern physics of magnetism.

We are very thankful to the organizers for their kind invitation to participate in the special issue dedicated to Dzyaloshinskii. In this short review we present our view on the fast growing field of DMI based mostly on

* E-mail: vmazurenko2011@gmail.com

our own experience of calculations and analysis of DMI parameters for specific magnetic materials.

2. Methods for calculating the Dzyaloshinskii–Moriya interaction. In this section, numerical approaches for calculating DMI are discussed. We start with a microscopic theory by Moriya [2] and show how it can be extended to analyze the dependence of DMI sign on the occupation of the $3d$ shell. Then we will focus on a correlated band theory of the DMI, that is free from basic limitations of the superexchange theory and can be applied in a wide range of electronic Hamiltonian parameters corresponding to insulators and metals. The last subsection of the methodological part is devoted to first-principles approaches based on the density functional theory.

2.1. Microscopic theory of DMI. The first microscopic theory of the antisymmetric anisotropic exchange interaction was developed by Moriya in 1960 and presented in Ref. [2]. It is based on the Anderson's idea on superexchange interaction [9] and formulated on the basis of the simplest electronic model accounting the on-site Coulomb interaction and the spin-orbit coupling on the level of the hopping integrals. Such an electronic model can be written in the following form

$$\hat{\mathcal{H}} = \sum_{ij,\sigma\sigma'} t_{ij}^{\sigma\sigma'} \hat{a}_{i\sigma}^{\dagger} \hat{a}_{j\sigma'} + \frac{1}{2} \sum_{i,\sigma\sigma'} U\, \hat{a}_{i\sigma}^{\dagger} \hat{a}_{i\sigma'}^{\dagger} \hat{a}_{i\sigma'} \hat{a}_{i\sigma}, \quad (2)$$

where $\hat{a}_{i\sigma}^{\dagger}(a_{i\sigma})$ are the creation (annihilation) operators. U is local Coulomb interaction, $t_{ij}^{\sigma\sigma'}$ is the element of the spin-resolved hopping matrix. Formally, Eq. (2) is nothing but the Hubbard model [10–12] that was officially introduced three years later in 1963. In the limit when the on-site Coulomb interaction is much larger than the hopping integrals such a Hubbard model can be reduced to the spin model

$$\hat{\mathcal{H}}^{spin} = \sum_{ij} J_{ij} \hat{\mathbf{S}}_i \hat{\mathbf{S}}_j + \sum_{ij} \mathbf{D}_{ij} [\hat{\mathbf{S}}_i \times \hat{\mathbf{S}}_j] + \\ + \sum_{ij} \hat{\mathbf{S}}_i \overleftrightarrow{\Gamma}_{ij} \hat{\mathbf{S}}_j, \quad (3)$$

where $\hat{\mathbf{S}}$ is the spin operator, J_{ij}, $\mathbf{D}_{ij}$ and $\overleftrightarrow{\Gamma}_{ij}$ are the isotropic exchange interaction, antisymmetric anisotropic (Dzyaloshinskii–Moriya) and symmetric anisotropic interactions, respectively. The summation runs twice over all pairs. In terms of the Hubbard Hamiltonian parameters the resulting expression for the DMI has the following form [2, 13]:

$$\mathbf{D}_{ij} = -\frac{i}{2U} [\mathrm{Tr}_\sigma\{\hat{t}_{ji}\}\mathrm{Tr}_\sigma\{\hat{t}_{ij}\boldsymbol{\sigma}\} - \\ - \mathrm{Tr}_\sigma\{\hat{t}_{ij}\}\mathrm{Tr}_\sigma\{\hat{t}_{ji}\boldsymbol{\sigma}\}], \quad (4)$$

where $\boldsymbol{\sigma}$ are the Pauli matrices.

Interestingly, the Moriya's microscopic theory was published in 1960, however, its first application to quantitative analysis of the magnetic properties of real materials was only done 30 years later by Coffey, Rice, and Zhang in Ref. [14]. They have estimated $\mathbf{D}_{ij}$ for different phases of La_2CuO_4 and $YBa_2Cu_3O_6$ compounds. It was shown that peculiarities in the crystal structures of these systems result in different patterns of the DMI vectors, and as the result different ground states with and without net magnetic moment can be realized.

An important feature of the one-band consideration of the DMI is that the Moriya's results were obtained by using an assumption of the constant U value without orbital dependence as well as by neglecting the intra-atomic (Hund's) exchange contribution. Further development of the microscopic theory of the antisymmetric anisotropic interaction was mainly related to its generalization to multi-orbital electronic Hamiltonians. As was shown in Ref. [13] inter-orbital Coulomb and intra-atomic exchange interactions play an important role in formation of the DMI.

Another important peculiarity of the one-band consideration of the DMI was demonstrated in Ref. [15]. It was shown that the resulting spin model, Eq. (3) is characterized by a specific symmetry of the symmetric anisotropic exchange interaction tensor, $\overleftrightarrow{\Gamma}_{ij}$ whose principal axis coincides with DMI for each bond. It means that the state of a system with weak ferromagnetism is higher in energy than the pure (compensated) antiferromagnetic state.

Despite of the above-mentioned and other limitations of the one-band approach for calculating magnetic interaction parameters, it provides a very simple and transparent way to analyze the properties of the interactions. For instance, it can be used for analysis of the dependence of the DMI sign on the occupation of the $3d$ shell experimentally observed in the series of isostructural weak ferromagnets, $MnCO_3$, $FeBO_3$, $CoCO_3$, and $NiCO_3$ as it was done by us in Ref. [16]. We consider the case of a transition metal oxide for which the crystal field splitting is much larger than the spin-orbit coupling, the latter can be treated as a perturbation. The corresponding expression for Dzyaloshinskii–Moriya interaction can be presented in the following form

$$\mathbf{D}_{ij}^{nn'} = \frac{4i}{U} [b_{ij}^{nn'} \mathbf{C}_{ji}^{n'n} - \mathbf{C}_{ij}^{nn'} b_{ji}^{n'n}], \quad (5)$$

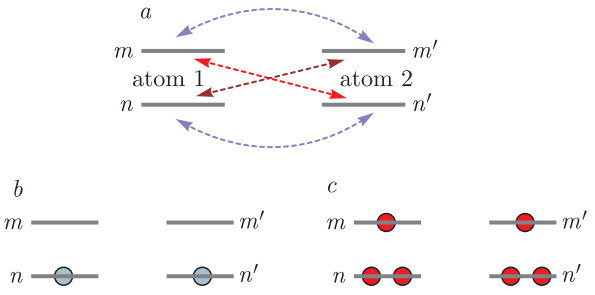

Fig. 1. (Color online) *a*) Minimal tight-binding model used for explaining the DMI sign change at variation of the occupation. The horizontal lines represent the electron levels and hoppings are shown with arrows. *b, c*) Two antiferromagnetic ground states corresponding to the $S = 1/2$ case, obtained in the model for different orbital fillings: $N = 2$ (*b*) and $N = 6$ (*c*)

where $b_{ij}^{nn'}$ is the (unperturbed) hopping integral between n-th ground orbital state of i-th atom and n'-th orbital state of j-th atom, $\mathbf{C}_{ij}^{nn'}$ is the corresponding hopping renormalized by SOC and U is the on-site Coulomb interaction. Thus, $\mathbf{C}_{ji}^{n'n}$ is given by

$$\mathbf{C}_{ji}^{n'n} = -\frac{\lambda}{2}\left[\frac{(\mathbf{L}_j^{m'n'})^*}{\epsilon_j^{m'} - \epsilon_j^{n'}} b_{ji}^{m'n} + \frac{\mathbf{L}_i^{mn}}{\epsilon_i^{m} - \epsilon_i^{n}} b_{ji}^{n'm}\right], \qquad (6)$$

where λ is the spin-orbit coupling constant, $\mathbf{L}_i^{mn}$ is the matrix element of the orbital angular momentum between the single m-th excited state and the n-th ground state Wannier functions which are centered at i-th ion, while ϵ_i^n represents the energy of the n-th Wannier orbital at the i-th ion.

Tight-binding model we considered contains two atoms having non-degenerate (n and n') and high-energy (m and m') levels. The schematic visualization of the model with the allowed hopping paths is presented in Fig. 1. In the simplest case one can assume that the same hopping integrals between high-energy (m and m') and low-energy (n and n') levels, $b_{12}^{m\,m'} = b_{12}^{n\,n'}$. The hoppings between orbitals of different symmetry require more detail analysis, since they define the DMI in the system in question. We assume that the geometry of the model system is fixed, which means that hopping integrals do not change with variation of the occupation.

Our tight-binding model has two ground states with different occupations N that correspond to the $S = 1/2$ case: $N = 2$ and $N = 6$ (Fig. 1). In the case $N = 2$, the ground state magnetic orbital is of symmetry $n(n')$, while for $N = 6$ it is $m(m')$. Another difference between these configurations is the different occupation of the excited states: they are empty and fully occupied for $N = 2$ and $N = 6$, respectively.

The difference between DMIs obtained for a system with two and six electrons is related to the difference between $\mathbf{C}_{21}^{n'\,n}$ and $\mathbf{C}_{21}^{m'\,m}$,

$$\mathbf{C}_{ji}^{n'\,n} = -\mathbf{C}_{ji}^{m'\,m} = -\frac{\lambda \mathbf{L}^{mn}}{2\Delta E}\left(b_{ji}^{m'\,n} - b_{ji}^{n'\,m}\right), \qquad (7)$$

where $\Delta E = \epsilon_i^n - \epsilon_i^m$.

It means that $\mathbf{D}_{ij}^{nn'}$ (for the system with two electrons) and $\mathbf{D}_{ij}^{mm'}$ (with six electrons) are of different signs. Thus, on the level of Moriya's approach, the sign of the DMI depends on the occupation of the excited states. Depending on the symmetry and occupation, each pair of $3d$ orbitals can result in positive or negative contribution to the total DMI between two atoms. It should be noted that similar dependence of the DMI sign on the occupation of the $3d$ shell can be also found in some series of metallic systems. In this sense interesting methodological results were obtained in Refs. [17–19].

It is important to discuss the limits of the Moriya's theory of DMI from the point of view of its using to study real physical systems. In its original formulation it is limited to the systems with the spin state of $S = 1/2$. Real transition metal compounds and nanosystems are of multi-orbital nature. In this case, the main question is how to define the numerous hopping and Coulomb interaction parameters of the Hubbard model. In principle, one can use approximations of different types to define the parameters [20, 21] by using available experimental data. Another approach is based on performing density functional theory (DFT) calculations and their parametrization using wannierization procedure developed in Refs. [22, 23] to construct the Wannier functions [24]. Then, on this basis the electronic model parameters are calculated. The most accurate numerical scheme to estimate local (U) and non-local Coulomb interaction parameters taking screening effects into account is based on the constrained random phase approximation [25].

The situation becomes even more complicated if one simulates a compound with a strong spin-orbit coupling. For this case effective numerical schemes based on the superexchange theory can be found in Refs. [26, 27].

2.2. Correlated band theory for DMI. We start with correlated band theory of DMI developed by us in Ref. [28]. It is based on the consideration of the general Hamiltonian of interacting electrons in a crystal:

$$\hat{H} = \sum_{12} c_1^\dagger t_{12} c_2 + \frac{1}{2}\sum_{1234} c_1^\dagger c_2^\dagger U_{1234} c_3 c_4, \qquad (8)$$

where $1 = (i_1, m_1, \sigma_1)$ is the set of site (i_1), orbital (m_1) and spin (σ_1) quantum numbers and t_{12} are hopping integrals that contain the spin-orbit coupling. These transfer couplings can be found by the Wannier-parameterization of the first-principle band structure with the spin-orbit coupling.

We will take into account only the local Hubbard-like interactions, keeping in $\hat{H}_u$ only terms with $i_1 = i_2 = i_3 = i_4$. This assumption corresponds to the DFT+U Hamiltonian [29] that is also a starting point for the DFT+DMFT (Dynamical Mean-Field Theory) [30–32]. It is crucially important for the later consideration that the interaction term $\hat{H}_u$ is supposed to be rotationally invariant.

We start with a collinear magnetic configuration, for instance an antiferromagnetic state, which is close to the real ground state (weak ferromagnet), but does not coincide with it due to the DMI. Let us re-define the DM Hamiltonian (Eq. (1)) in a slightly different way:

$$H_{DMI} = \sum_{ij} \mathbf{D}'_{ij}[\mathbf{e}_i \times \mathbf{e}_j], \tag{9}$$

where $\mathbf{e}_i$ is a unit vector in the direction of the i-th site magnetic moment and $\mathbf{D}'_{ij}$ is the Dzyaloshinskii–Moriya vector. We analyze the magnetic configuration that is slightly deviated from the collinear state,

$$\mathbf{e}_i = \eta_i \mathbf{e}_0 + [\delta\boldsymbol{\phi}_i \times \eta_i \mathbf{e}_0], \tag{10}$$

where $\eta_i = \pm 1$, $\mathbf{e}_0$ is the unit vector along the vector of antiferromagnetism, and $\delta\boldsymbol{\phi}_i$ are the vectors of small angular rotations.

Substituting Eq. (10) into Eq. (9) one finds for the variation of the magnetic energy:

$$\delta E = \sum_{ij} \mathbf{D}'_{ij}(\delta\boldsymbol{\phi}_i - \delta\boldsymbol{\phi}_j). \tag{11}$$

Now we should calculate the same variation for the microscopic Hamiltonian (8). Similar to the procedure used in Ref. [33] to derive exchange interactions for the LDA+DMFT approach, we consider the effect of the local rotations

$$\hat{R}_i = e^{i\delta\boldsymbol{\varphi}_i \hat{\mathbf{J}}_i}, \tag{12}$$

on the total energy; here $\hat{\mathbf{J}}_i = \hat{\mathbf{L}}_i + \hat{\mathbf{S}}_i$ is the total moment operator, $\hat{\mathbf{L}}_i$ and $\hat{\mathbf{S}}_i$ are the orbital and spin moments, respectively.

The resulting DMI is given by anticommutator of $\hat{\mathbf{J}}$ and $\hat{t}_{ij}$:

$$\mathbf{D}'_{ij} = -\frac{i}{2}\mathrm{Tr}_{m,\sigma} N_{ji}[\hat{\mathbf{J}}, \hat{t}_{ij}]_+, \tag{13}$$

where

$$N_{ji} = \langle c_i^\dagger c_j \rangle = -\frac{1}{\pi}\int\limits_{-\infty}^{E_f} \mathrm{Im}\, G_{ji}(E)\, dE$$

is the inter-site occupation matrix and $\hat{G}$ is the Green function of the system, E_F is the Fermi energy. The occupation matrix can be calculated by using a static (such as DFT+U [29]) or a dynamic mean-field approach (DFT+DMFT [30–32]).

Note that the occupation matrix is calculated in the corresponding collinear states, which strictly speaking can be done self-consistently only within constrained calculations [34]. Using the decomposition of the total moment $\hat{\mathbf{J}}$ into orbital and spin moments, we have a natural representation of the Dzyaloshinskii–Moriya vector (13) as a sum of the orbital and spin contributions which are related with the rotations in orbital and spin space, respectively.

The resulting expression Eq. (13) is of general nature and its spin part can be also derived in the case of the metallic systems as it was shown in [35].

2.3. DFT-based methods. In this section we discuss mean-field approaches for calculating the DMI that are realized on the basis of the numerical methods of the density functional theory. The net DMI can be assessed by calculating the DFT total energies for the two sets of spin spiral states having opposite helicities [36–38] or by using Berry phase theory [39]. In order to calculate the individual pair-wise DMI, one can employ the magnetic force theorem [40]. According to this theorem, the variation of the total energy of the system due to a magnetic excitation can be expressed through the variation of the single-particle energy.

In $3d$ systems, the spin-orbit coupling in itself can be also considered as a perturbation [41, 42]. One can consider a mixed perturbation scheme with respect to the rotation and spin-orbit coupling, which leads to the antisymmetric anisotropic DMI [43]

$$D_{ij}^z = -\frac{1}{8\pi S_i S_j}\,\mathrm{Re}\int\limits_{-\infty}^{E_F} d\epsilon \times$$
$$\times \sum_k \mathrm{Tr}_m(\Delta_i G_{ik}^{\downarrow} H_{k\downarrow\downarrow}^{so} G_{kj}^{\downarrow} \Delta_j G_{ji}^{\uparrow} -$$
$$- \Delta_i G_{ik}^{\uparrow} H_{k\uparrow\uparrow}^{so} G_{kj}^{\uparrow} \Delta_j G_{ji}^{\downarrow} + \Delta_i G_{ij}^{\downarrow} \Delta_j G_{jk}^{\uparrow} H_{k\uparrow\uparrow}^{so} G_{ki}^{\uparrow} -$$
$$- \Delta_i G_{ij}^{\uparrow} \Delta_j G_{jk}^{\downarrow} H_{k\downarrow\downarrow}^{so} G_{ki}^{\downarrow}). \tag{14}$$

Other components of the Dzyaloshinskii–Moriya vector for particular bond can be obtained from the z ones by

rotation of the coordinate system. Similar expression for DMI was obtained by Solovyev et al. [44].

We have applied the developed method for calculating the DMI to give a microscopic explanation to the scanning tunneling microcopy experiments performed for chains of manganese atoms on CuN surface [43]. Weak ferromagnetism due to the DMI between neighbouring manganese atoms was predicted. Another important example is a first-principles study of the molecular nanomagnet Mn_{12} for which most theoretical works on molecular magnets are mainly relied on the so-called rigid-spin model. Within such a model a complex system of interacting spins is replaced by just one big spin, with some magnetic anisotropy being introduced artificially. However, such a description is rather simplistic and largely ignores intermolecular interactions. Previously, it was predicted that the DMI plays a crucial role in the physics of molecular magnets [45] and in particular magnetic tunneling effects in Mn_{12} [46]. In our work [47] we have demonstrated that the account of the inter-atomic anisotropic exchange interactions in Mn_{12} gives opportunity to reproduce excitation energies observed in the inelastic neutron scattering experiments for this system.

In the case of the systems with strong spin-orbit coupling one could still use similar Green's function approach within the magnetic force theorem [48]. The expressions for DMI, which do not rely on the smallness of spin-orbit coupling constant have been derived independently by several groups [49–53].

3. Applications.

3.1. Weak ferromagnetism in antiferromagnets. Discovery of the weak ferromagnetism in iron hematite, Fe_2O_3 (Ref. [54, 55]) was the starting point for development of the DMI theory. More specifically, Fe_2O_3 is pure antiferromagnet with magnetic moments parallel to the trigonal axis c at $T < 260$ K. In the temperature range between 260 and 950 K, the magnetic moments are in-plane and a small canting of the magnetic moment exists. As the result of this canting there is net magnetic moment in the antiferromagnetic system. The weak ferromagnetism in Fe_2O_3 was explored with first-principles DFT calculations in Ref. [56] and with Green's function approach based on the magnetic force theorem in Ref. [57].

A more interesting situation concerning weak ferromagnetism in antiferromagnets is observed in transition metal oxides having calcite structure. Previous magnetization measurements [58–61] have confirmed the existence of the non-compensate in-plane magnetization in several materials of this kind. However, the precise direction of the weak ferromagnetic moment with respect to the crystallographic axes and hence the "sign" of DM interaction remained unknown. For the first time, this was unambiguously identified for $FeBO_3$ using resonant x-ray diffraction in Ref. [62]. We have performed *ab initio* calculations and extracted the DM vectors using Eq. (13). It was found that the theoretical calculations do not only reproduce the correct sign of DM vectors, but also give a very good estimate of the canting angle.

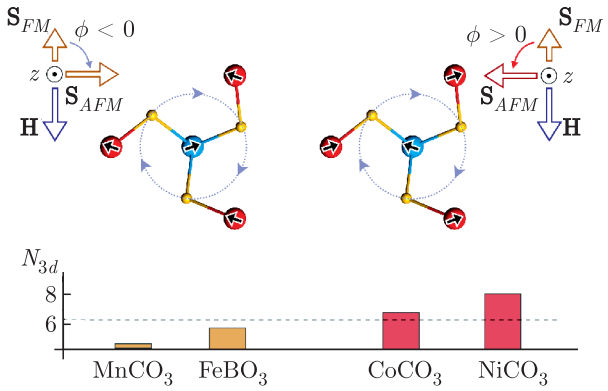

Fig. 2. (Color online) Local atomic and magnetic orders in the weak ferromagnets. The ions of the two magnetic sublattices are represented by blue (site 1) and red (site 2) spheres, with black arrows denoting the direction of their spins. Oxygen atoms between the two adjacent transition metal layers are represented as yellow spheres. The dotted circles highlight the twist of the oxygen layer. The bottom panel shows the occupation of the $3d$ level of a magnetic ion. The left and right panels show the two possible magnetic configurations which stabilize depending on the $3d$ occupation and, therefore, the sign of the DMI, for a net ferromagnetic moment pointing along the magnetic field $\mathbf{H}$. $\mathbf{S}_{AFM}$ denotes the direction of the antiferromagnetic spin structure. This figure is reproduced with permission from Ref. [16]

Next, we addressed the series of isostructural calcite oxides, namely: $MnCO_3$, $FeBO_3$, $CoCO_3$, $NiCO_3$. They all exhibit weak ferromagnetism and experiments based on the technique developed in Ref. [62], have revealed the change of canting angle sign across the series [16]. More specifically, the compounds $MnCO_3$ and $FeBO_3$ are characterized by the rotation sense which differs from that for the $CoCO_3$ and $NiCO_3$ systems. It is schematically shown in Fig. 2. Taking into account that these compounds have the same crystal structure (and the same crystallographic chirality), such a sign change can be attributed to the difference in the occupation of the $3d$ shell.

To provide a theoretical support to these experiments in Ref. [16] we have performed first-principles calculations within local density approximation taking

into account the on-site Coulomb interaction U and spin-orbit coupling (DFT+U+SO). The resulting magnetic configuration is antiferromagnetic one characterized by a canting of the magnetic moments. Such a canted state is the lowest-energy state for all the systems under consideration. The calculated magnitudes and signs of the canting angles are in good agreement with experimental data. However, the full calculation does not provide a truly microscopic understanding of the DMI sign change phenomena. For that a minimal tight-binding model based on the Moriya's theory as described in the methodological part of this paper becomes extremely useful.

3.2. Magnetic skyrmions. Investigation of skyrmions is a widely studied topic in the modern material science [63–71]. Previous experimental and theoretical studies on the topologically-protected magnetic skyrmion excitations were fully focused on the transition metal crystals and nanosystems. This seems to be natural, since these materials are characterised by well-localised magnetic moments originated from the partially-filled $3d$ states and magnetic anisotropy [72,73] that facilitates an experimental detection of the distinct magnetic textures. In works [74–76] a new class of materials, surface nanostructures with *sp* element revealing skyrmion excitations at experimentally achievable magnetic fields and temperatures was introduced. The non-trivial result, that such *sp*-electron systems are, in principle, characterized by a magnetic state, was experimentally confirmed in Refs. [77–79].

Our first-principles calculations [74–76] have confirmed a long-range character of the magnetic states in graphene derivatives C_2H and C_2F as well as in surface nanostructures Si(111):{C, Si, Sn, Pb} and in Sn on SiC(0001). The corresponding Wannier functions in these systems demonstrate that substantial amount of the electron density is concentrated in the interstitial region. In all the cases we have found that the values of the calculated hopping integrals are much smaller than that of the Coulomb interactions, which gives us opportunity to construct a Heisenberg-type Hamiltonian for the localized spins $S = 1/2$ within the superexchange theory.

The constructed spin models for graphene derivatives, Si(111):{C, Si, Sn, Pb} and Sn monolayer on SiC(0001) surface were solved by means of the Monte Carlo methods, which gives us opportunity to define the magnetic phases of these materials depending on the external magnetic field and temperature. It was found that one can stabilize skyrmionic solutions in the case of the semifluorinated graphene (Fig. 3)

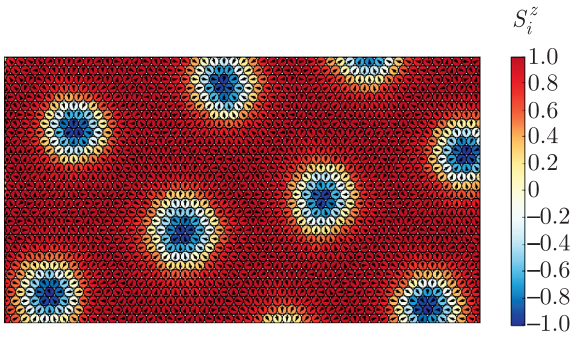

Fig. 3. (Color online) Skyrmionic magnetic structure obtained from the Monte Carlo simulations for C_2F system. This figure is adopted from Ref. [74]

and nanosystems with heavy adatoms Sn/Si(111), Pb/Si(111) and Sn/SiC(0001). The key quantity here allowing the formation of the topologically protected magnetic structures is the anisotropic Dzyaloshinskii–Moriya interaction.

4. Perspectives. Despite there were several decades of intensive investigations on DMI and related phenomena we think that this is still young and very promising research field within which one could focus on the following directions for future investigations. From the very beginning DMI is considered as a representative of one of the smallest energy scales in the magnetic Hamiltonians of the strongly correlated systems, $|\mathbf{D}_{ij}| \ll J_{ij}$. It is due to the DMI always contains additional relativistic small parameter, the ratio of electron velocity in atoms to the velocity of light. However, such a dominance of the Heisenberg exchange interaction can be overcome by different means. For instance, manipulation of magnetic interactions via a strong periodic in time electromagnetic field [80] ("Floquet engineering") suggests that using real nanosystems and real values of the laser fields one can reach the regime when the Heisenberg exchange J_{ij} is arbitrarily small, or even equal to zero, whereas the Dzyaloshinskii–Moriya parameter $\mathbf{D}_{ij}$ remains constant. As an interesting example of such a situation, a new class of two-dimensional Heisenberg-exchange-free materials where a completely new type of skyrmions (Fig. 4) that emerge as the result of the competition between the DMI and uniform magnetic field has been introduced [81].

Another fascinating research field is related to a quantum skyrmions that in contrast to the classical counterpart are practically unexplored. The main methodological problem here is how to characterize the topology of quantum system with a three-dimensional magnetic structure when the orientation of a spin is

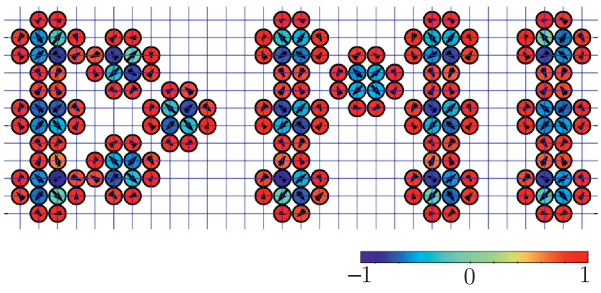

Fig. 4. (Color online) Abbreviation of Dzyaloshinskii–Moriya interaction written with nanoskyrmions. This is a result of Monte Carlo simulations of the Heisenberg-exchange-free model on the square lattice with non-regular site occupation. Arrows and colors depict the in-plane and out-of-plane spin projections, respectively

ill-defined. One of the possible solutions was recently proposed by some of us in Ref. [82] where scalar chirality operator was introduced to define a quantum analog of the topological charge.

The other direction we consider to be very attractive is DMI applications in quantum computing. Existence of the anisotropic exchange interactions between qubits can be used for preparing highly entangled quantum states that play an important role in quantum information processing [83, 84]. The future of DMI looks bright and promising.

Funding. The work of A. I. L. and M. I. K. is supported by European Research Council via Synergy Grant 854843–FASTCORR. Y. O. K. acknowledges the financial support from the Swedish Research Council (VR) under the project No. 2019-03569. The work of V. V. M. was supported by Act 211 Government of the Russian Federation, contract 02.A03.21.0006.

The full text of this paper is published in the English version of JETP.

REFERENCES

1. I. Dzyaloshinskii, J. Phys. Chem. Sol. **4**, 241 (1958).

2. T. Moriya, Phys. Rev. **120**, 91 (1960); T. Moriya, in *Magnetism*, Vol. I, ed. by G. T. Rado and H. Suhl, Acad. Press, New York (1963), p. 86.

3. H. Katsura, N. Nagaosa, and A. V. Balatsky, Phys. Rev. Lett. **95**, 057205 (2005).

4. I. A. Sergienko and E. Dagotto, Phys. Rev. B **73**, 094434 (2006).

5. S. W. Cheong and M. Mostovoy, Nature Mater. **6**, 13 (2007).

6. M. Bode, M. Heide, K. von Bergmann, P. Ferriani, S. Heinze, G. Bihlmayer, A. Kubetzka, O. Pietzsch, S. Blügel, and R. Wiesendanger, Nature **447**, 190 (2007).

7. M. Heide, G. Bihlmayer, and S. Blügel, Phys. Rev. B **78**, 140403(R) (2008).

8. S. Rohart and A. Thiaville, Phys. Rev. B **88**, 184422 (2013).

9. P. W. Anderson, Phys. Rev. **115**, 2 (1959).

10. J. Hubbard, Proc. Roy. Soc. A **276**, 238 (1963).

11. M. C. Gutzwiller, Phys. Rev. Lett. **10**, 159 (1963).

12. J. Kanamori, Prog. Theor. Phys. **30**, 275 (1963).

13. T. Yildirim, A. B. Harris, A. Aharony, and O. Entin-Wohlman, Phys. Rev. B **52**, 10239 (1995).

14. D. Coffey, T. M. Rice, and F. C. Zhang, Phys. Rev. B **44**, 10112 (1991).

15. L. Shekhtman, O. Entin-Wohlman, and A. Aharony, Phys. Rev. Lett. **69**, 836 (1992).

16. G. Beutier, S. P. Collins, O. V. Dimitrova, V. E. Dmitrienko, M. I. Katsnelson, Y. O. Kvashnin, A. I. Lichtenstein, V. V. Mazurenko, A. G. A. Nisbet, E. N. Ovchinnikova, and D. Pincini, Phys. Rev. Lett. **119**, 167201 (2017).

17. A. Fert and P. M. Levy, Phys. Rev. Lett. **44**, 1538 (1980).

18. V. Kashid, T. Schena, B. Zimmermann, Y. Mokrousov, S. Blügel, V. Shah, and H. G. Salunke, Phys. Rev. B **90**, 054412 (2014).

19. A. Belabbes, G. Bihlmayer, F. Bechstedt, S. Blügel, and A. Manchon, Phys. Rev. Lett. **117**, 247202 (2016).

20. A. S. Moskvin, M. A. Vigura, and A. P. Agafonov, Sov. Phys. Solid State **28**, 1631 (1986).

21. A. Moskvin, J. Magn. Magn. Mater. **400**, 117 (2016), Proc. of the 20th Int. Conf. on Magnetism, Barcelona (2015).

22. N. Marzari and D. Vanderbilt, Phys. Rev. B **56**, 12847 (1997).

23. N. Marzari, A. A. Mostofi, J. R. Yates, I. Souza, and D. Vanderbilt, Rev. Mod. Phys. **84**, 1419 (2012).

24. A. A. Mostofi, J. R. Yates, G. Pizzi, Y.-Su. Lee, I. Souza, D. Vanderbilt, and N. Marzari, Comput. Phys. Commun. **185**, 2309 (2014).

25. F. Aryasetiawan, K. Karlsson, O. Jepsen, and U. Schönberger, Phys. Rev. B **74**, 125106 (2006).

26. I. V. Solovyev, New J. Phys. **11**, 093003 (2009).

27. I. V. Solovyev, V. V. Mazurenko, and A. A. Katanin, Phys. Rev. B **92**, 235109 (2015).

28. M. I. Katsnelson, Y. O. Kvashnin, V. V. Mazurenko, and A. I. Lichtenstein, Phys. Rev. B **82**, 100403(R) (2010).

29. V. I. Anisimov, F. Aryasetiawan, and A. I. Lichtenstein, J. Phys.: Condens. Matter **9**, 767 (1997).

30. A. I. Lichtenstein and M. I. Katsnelson, Phys. Rev. B **57**, 6884 (1998).

31. G. Kotliar, S. Y. Savrasov, K. Haule, V. S. Oudovenko, O. Parcollet, and C. A. Marianetti, Rev. Mod. Phys. **78**, 865 (2006).

32. V. Anisimov, A. Poteryaev, M. Korotin, A. Anokhin, and G. Kotliar, J. Phys.: Condens. Matter **9**, 7359 (1997).

33. M. I. Katsnelson and A. I. Lichtenstein, Eur. Phys. J. B **30**, 9 (2002).

34. G. M. Stocks, B. Ujfalussy, X. D. Wang, D. M. C. Nicholson, W. A. Shelton, Y. Wang, A. Canning, and B. L. Gyorffy, Phil. Mag. B **78**, 665 (1998).

35. T. Kikuchi, T. Koretsune, R. Arita, and G. Tatara, Phys. Rev. Lett. **116**, 247201 (2016).

36. H. Yang, A. Thiaville, S. Rohart, A. Fert, and M. Chshiev, Phys. Rev. Lett. **115**, 267210 (2015).

37. B. Zimmermann, G. Bihlmayer, M. Böttcher, M. Bouhassoune, S. Lounis, J. Sinova, S. Heinze, S. Blügel, and B. Dupé, Phys. Rev. B **99**, 214426 (2019).

38. L. M. Sandratskii, Phys. Rev. B **96**, 024450 (2017).

39. F. Freimuth, S. Blügel, and Y. Mokrousov, J. Phys.: Condens. Matter **26**, 104202 (2014).

40. A. I. Liechtenstein, M. I. Katsnelson, V. P. Antropov, and V. A. Gubanov, J. Magn. Magn. Mater. **67**, 65 (1987).

41. P. Bruno, Phys. Rev. B **39**, 865 (1989).

42. I. V. Solovyev, P. H. Dederichs, and I. Mertig, Phys. Rev. B **52**, 13419 (1995).

43. A. N. Rudenko, V. V. Mazurenko, V. I. Anisimov, and A. I. Lichtenstein, Phys. Rev. B **79**, 144418 (2009).

44. I. Solovyev, N. Hamada, and K. Terakura, Phys. Rev. Lett. **76**, 4825 (1996).

45. M. I. Katsnelson, V. V. Dobrovitski, and B. N. Harmon, Phys. Rev. B **59**, 6919 (1999).

46. H. A. De Raedt, A. H. Hams, V. V. Dobrovitski, M. Al-Saqer, M. I. Katsnelson, and B. N. Harmon, J. Magn. Magn. Mater. **246**, 392 (2002).

47. V. V. Mazurenko, Y. O. Kvashnin, Fengping Jin, H. A. De Raedt, A. I. Lichtenstein, and M. I. Katsnelson, Phys. Rev. B **89**, 214422 (2014).

48. M. I. Katsnelson and A. I. Lichtenstein, Phys. Rev. B **61**, 8906 (2000).

49. L. Udvardi, L. Szunyogh, K. Palotás, and P. Weinberger, Phys. Rev. B **68**, 104436 (2003).

50. H. Ebert and S. Mankovsky, Phys. Rev. B **79**, 045209 (2009).

51. A. Secchi, A. Lichtenstein, and M. Katsnelson, Ann. Phys. **360**, 61 (2015).

52. S. Mankovsky and H. Ebert, Phys. Rev. B **96**, 104416 (2017).

53. Y. O. Kvashnin, A. Bergman, A. I. Lichtenstein, and M. I. Katsnelson, Phys. Rev. B **102**, 115162 (2020).

54. T. Smith, Phys. Rev. **8,** 721 (1916); L. Neel, Rev. Mod. Phys. **25,** 58 (1953).

55. S. V. Vonsovsky, *Magnetism*, Vol. 2, Wiley, New York (1974).

56. L. M. Sandratskii, M. Uhl, and J. Kübler, J. Phys.: Condens. Matter **8**, 983 (1996); L. M. Sandratskii and J. Kübler, Europhys. Lett. **33**, 447 (1996).

57. V. V. Mazurenko and V. I. Anisimov, Phys. Rev. B **71**, 184434 (2005).

58. A. Kosterov, T. Frederichs, and T. von Dobeneck, Phys. Earth Planet. Interiors **154**, 234 (2006), Developments in Techniques and Methods Related to Rock Magnetism.

59. M. P. Petrov, G. A. Smolensky, A. P. Paugurt, and S. A. Kizhaev, AIP Conf. Proc. **5**, 379 (1972).

60. A. S. Borovik-Romanov and V. I. Ozhogin, Sov. Phys. JETP **12**, 18 (1961).

61. N. M. Kreines and T. A. Shal'nikova, Sov. Phys. JETP **31**, 280 (1970).

62. V. E. Dmitrienko et al., Nature Phys. **10**, 202 (2014).

63. A. N. Bogdanov and D. A. Yablonskii, Sov. Phys. JETP **68**, 101 (1989).

64. S. Mühlbauer, B. Binz, F. Jonietz, C. Pfleiderer, A. Rosch, A. Neubauer, R. Georgii, and P. Böni, Science **323**, 915 (2009).

65. A. Neubauer, C. Pfleiderer, B. Binz, A. Rosch, R. Ritz, P. G. Niklowitz, and P. Böni, Phys. Rev. Lett. **102**, 186602 (2009).

66. W. Münzer, A. Neubauer, T. Adams, S. Mühlbauer, C. Franz, F. Jonietz, R. Georgii, P. Böni, B. Pedersen, M. Schmidt, A. Rosch, and C. Pfleiderer, Phys. Rev. B **81**, 041203 (2010).

67. X. Z. Yu, Y. Onose, N. Kanazawa, J. H. Park, J. H. Han, Y. Matsui, N. Nagaosa, and Y. Tokura, Nature **465**, 901 (2010).

68. N. Nagaosa and Y. Tokura, Nature Nanotechnol. **8**, 899 (2013).

69. O. Janson, I. Rousochatzakis, A. A. Tsirlin, M. Belesi, A. A. Leonov, U. K. Rößler, J. van den Brink, and H. Rosner, Nature Commun. **5**, 5376 (2014).

70. S. Heinze, K. von Bergmann, M. Menzel, J. Brede, A. Kubetzka, R. Wiesendanger, G. Bihlmayer, and S. Blügel, Nature Phys. **7**, 713 (2011).

71. N. Romming, C. Hanneken, M. Menzel, J. E. Bickel, B. Wolter, K. von Bergmann, A. Kubetzka, and R. Wiesendanger, Science **341**, 636 (2013).

72. I. Beljakov, V. Meded, F. Symalla, K. Fink, S. Shallcross, M. Ruben, and W. Wenzel, Nano Lett. **14**, 3364 (2014).

73. E. Torun, H. Sahin, C. Bacaksiz, R. T. Senger, and F. M. Peeters, Phys. Rev. B **92**, 104407 (2015).

74. V. V. Mazurenko, A. N. Rudenko, S. A. Nikolaev, D. S. Medvedeva, A. I. Lichtenstein, and M. I. Katsnelson, Phys. Rev. B **94**, 214411 (2016).

75. D. I. Badrtdinov, S. A. Nikolaev, M. I. Katsnelson, and V. V. Mazurenko, Phys. Rev. B **94**, 224418 (2016).

76. D. I. Badrtdinov, S. A. Nikolaev, A. N. Rudenko, M. I. Katsnelson, and V. V. Mazurenko, Phys. Rev. B **98**, 184425 (2018).

77. S. Glass, G. Li, F. Adler, J. Aulbach, A. Fleszar, R. Thomale, W. Hanke, R. Claessen, and J. Schäfer, Phys. Rev. Lett. **114**, 247602 (2015).

78. G. Li, P. Höpfner, J. Schäfer, C. Blumenstein, S. Meyer, A. Bostwick, E. Rotenberg, R. Claessen, and W. Hanke, Nature Commun. **4**, 1620 (2013).

79. H. González-Herrero, J. M. Gómez-Rodríguez, P. Mallet, M. Moaied, J. José Palacios, C. Salgado, M. M. Ugeda, J.-Y. Veuillen, F. Yndurain, and I. Brihuega, Science **352**, 437 (2016).

80. E. A. Stepanov, C. Dutreix, and M. I. Katsnelson, Phys. Rev. Lett. **118**, 157201 (2017).

81. E. A. Stepanov, S. A. Nikolaev, C. Dutreix, M. I. Katsnelson, and V. V. Mazurenko, J. Phys.: Condens. Matter **31**, 17LT0 (2019).

82. O. M. Sotnikov, V. V. Mazurenko, J. Colbois, F. Mila, M. I. Katsnelson, and E. A. Stepanov, arXiv: 2004.13526.

83. L. K. Grover, Phys. Rev. Lett. **79**, 325 (1997).

84. P. W. Shor, SIAM J. Comput. **26**, 1484 (1997).